Geophys. J. R. astr. Soc. (1972) **31**, 3–25.

Scaling Law of Earthquake Source Time-Function

Keiiti Aki

(Received 1972 March 3)

Summary

Further evidences support the scaling law of far-field seismic spectrum based upon the ω-square model (Aki) for earthquakes with $M_s > 6$ and for periods $T > 10$ s. Recent observations, however, unequivocally require the modification of the above law for periods $T < 10$ s. Unfortunately, the presently available data are not sufficient for a unique revision of the scaling law. We propose two alternatives and discuss their implications and consequences. In either case, we have to conclude that a large earthquake and a small one are substantially different. One interesting feature of the ω-square model appears to be unaffected by the required revision; that is, the spectral density of the fault-slip time-function for periods $T < 5$ s takes the same absolute value, independent of magnitude, for earthquakes greater than $M_s = 6{\cdot}5$. This result has important consequences in earthquake engineering because the seismic motion in the vicinity of an earthquake fault will scale as the fault-slip motion.

1. Introduction

As a first step to relate the seismic spectrum with earthquake magnitude, a model of earthquake ensemble was proposed by Aki (1967) on the basis of a dislocation theory of earthquake faulting. In this model, the source factor of far-field spectrum diminishes inversely proportional to the square of frequency ω beyond a corner frequency. For this frequency dependence, it was called the 'ω-square model'. Below the corner frequency, the spectrum is flat with the height proportional to the seismic moment (Aki 1966). A family of such spectral curves was constructed on the assumption that large and small earthquakes are similar phenomena in a medium with given elastic constants and density. The assumption implies the same geometry, a constant stress-drop, constant rupture velocity and slip velocity, independent of magnitude, and it follows that the corner frequency is inversely proportional to the fault length, and the seismic moment to the cube of fault length. Thus, the corner frequency lies on a straight line with slope 3 in Fig. 1 which shows the logarithm of spectrum against the logarithm of period. The spacings between the curves are made equal at the period of 20 s to be compatible with the definition of M_s by Gutenberg & Richter. The scaling law shown in Fig. 1 explained very well Berckhemer's (1962) observations on spectral ratios, Gutenberg–Richter's (1956) $M_s - M_b$ relation for $M_s > 6$, and Tocher's (1960) data on the earthquake fault length and magnitude.

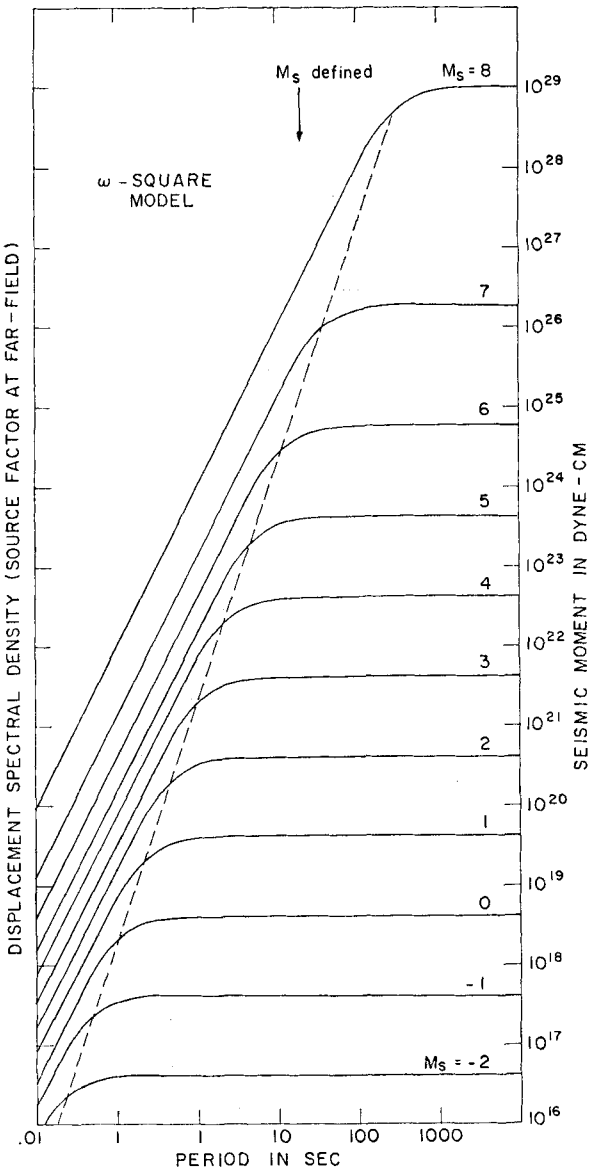

FIG. 1. Source factor of far-field seismic spectral density from earthquakes with various M_s for the ω-square model reproduced from Aki (1967).

The assumption of similarity comes from the idea advocated by Tsuboi (1940, 1956, 1958, 1965) who held the view that the strain energy density prior to the earthquake occurrence is the property of rock material independent of earthquake magnitude, and that the energy of an earthquake is determined by the volume within which it has been stored. This idea radically contradicts the assumption underlying Benioff's (1951) strain release curve, which was calculated as the square root of energy release implying a constant earthquake volume independent of magnitude. The latter view may be natural to the California seismologists, because the majority of California earthquakes, large or small, appear to be associated with the same fault plane; the San Andreas. It was, however, unacceptable to the Japanese seismologists

who were familiar with the distinct difference in spectral structure between large and small, especially microearthquakes (Asada 1957). The controversy appeared to have been settled when Båth & Duda (1964) summarized observational data in favour of Tsuboi's idea and proposed an improvement of Benioff's method for calculating the strain release curve. Thus, the assumption of similarity was the most reasonable one at the time when the ω-square model was proposed.

Since then, a large amount of observational data have become available for more critical testing of the proposed model. In general, the new evidences support the ω-square model for earthquakes larger than $M_s = 6$, and for periods longer than 10 s. For smaller earthquakes or for shorter periods, new evidences require revision of the ω-square model. The purpose of the present paper is to propose such a revision, and to discuss its implications and consequences. Since, unfortunately, the presently available data are not sufficient for a unique revision, discussion will be made for two alternative revision.

An interesting feature of the ω-square model is that the spectral density of fault-slip time-function for periods shorter than 5 s is identical, in the absolute scale, for all the earthquakes greater than $M_s = 6{\cdot}5$. This feature of the ω-square model, which is particularly important for earthquake engineering, is unaffected by the revision required in the present paper.

2. Comparison with observations

The validity of the scaling law shown in Fig. 1 can be tested against various kinds of observations. In general, the right half ($T > 10$ s) of Fig. 1 shows excellent agreements with the observed data, but the left half ($T < 10$ s) does not. Let us start with observations at the infinite period, that is, static fault parameters.

(1) *Fault length*

Fig. 2 shows the data on magnitude and fault length reproduced from Chinnery (1969). In view of the difficulties in extracting reliable observations of fault parameters from field data the observed points in Fig. 2 were thoughtfully limited to those

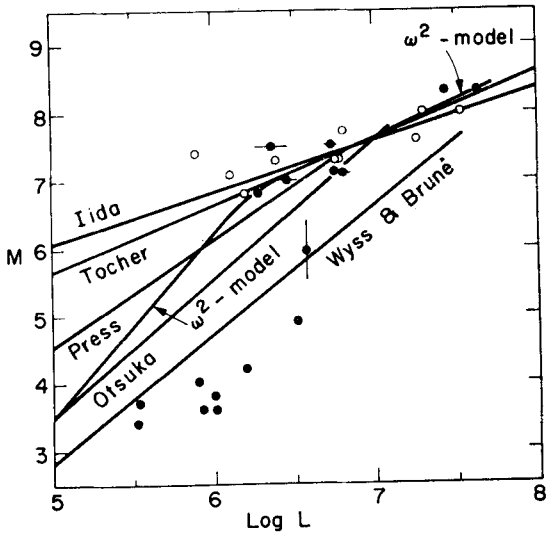

FIG. 2. Fault length L as a function of magnitude reproduced from Chinnery (1969) with the additional curve for the ω-square model. See text for the curves designated by the names of investigators.

of near-vertical faults on which the movement was predominantly strike-slip. The surface wave magnitude M_s is used for events with magnitude over 6, and local Richter magnitude M_L for events less than 6. The empirical formulas by Iida (1959, 1965) and Tocher (1958) show a good fit to the data for large earthquakes. Otsuka's (1965) formula is proposed to take into account the hidden part of a fault unnoticed by field observation. Both Otsuka's (1965) and Press' (1967) formula predict much steeper slope than observed for $M > 7$. This discrepancy was attributed to the non-similar fault shape between large and small earthquakes due to the effect of crustal structure.

The ω-square model, on the other hand, gives exactly the same slopes as those of the Iida and Tocher formulas, and explains the observed slope for large events excellently without invoking the non-similarity. The bending of the curve at about $M = 7$ is due to the inefficiency of M_s as a measure of the size of large earthquakes.

The curve for the ω-square model in Fig. 2 was drawn, first, by finding the relation between M_s and the corner period from Fig. 1, and then multiplying the corner period by a constant to obtain the fault length. Under the assumption of similarity, the corner period and fault length should be proportional to each other. The proportionality constant giving the best fit to observation is $0{\cdot}65\,\mathrm{km\,s^{-1}}$ (see Fig. 11 of Aki 1967). It is interesting to compare this value with the theoretical coefficient used by Brune (1970, 1971), in which the radius r of earthquake source is related to the corner frequency f_0 of shear wave spectra by $r = 2{\cdot}34\beta/2\pi f_0$, where β is the shear velocity. If we take $2r$ as the fault length, the coefficient is $2{\cdot}6\,\mathrm{km\,s^{-1}}$ for $\beta = 3{\cdot}5\,\mathrm{km\,s^{-1}}$. This is about 4 times larger than the value obtained from the observational data for large earthquakes. It appears that Brune's theory does not apply to large earthquakes. The discrepancy may be attributed to his assumption of infinite rupture velocity, which is not realistic for a spontaneous rupture (Ida & Aki 1972).

Within the scheme of Aki's (1967) statistical fault model, the corner period T is related to the mean free path k_L^{-1} of fault propagation by the relation

$$k_L^{-1} = \frac{v}{2\pi} T$$

where v is the velocity of rupture propagation. For $v = 3\,\mathrm{km\,s^{-1}}$, we find that the mean free path is proportional to the corner period with coefficient about 0·5, which is close to the observed coefficient 0·65 for the fault length. For large earthquakes and for long periods, therefore, the rupture propagation appears to be smooth and encounters no obstacle during the growth to its final length.

The curve based on the ω-square model does not explain the data for small earthquakes shown in Fig. 2, which includes the Imperial earthquake of 1966 March 4, described by Brune & Allen (1967) who demonstrated beyond doubt that an earthquake with magnitude 3·6 could have a 10 km fault length. However, some of the data are questionable. For example, one aftershock ($M = 4{\cdot}9$) of the Parkfield earthquake of 1966 was given a fault length of 33 km from creep observations (Wyss & Brune 1968). The wide-band spectra of Love waves (Filson & McEvilly 1967) from this earthquake, however, did not show the evidence for such a long fault. Since the field measurement of fault length becomes increasingly difficult with decreasing magnitude, we must resort to indirect methods. For example, Lieberman & Pomeroy (1970) used the data on an aftershock area in a general support of the Wyss–Brune curve of Fig. 2 . However, an accurate determination of aftershock area for a small main-shock is a difficult problem and also the aftershock area may give an overestimate of the main-shock fault area (Aki 1968).

(2) *Stress drop*

Further evidences from field data support the validity of the ω-square model for large earthquakes. Fig. 3 shows the relation between M_s and $\log LD^2$ reproduced

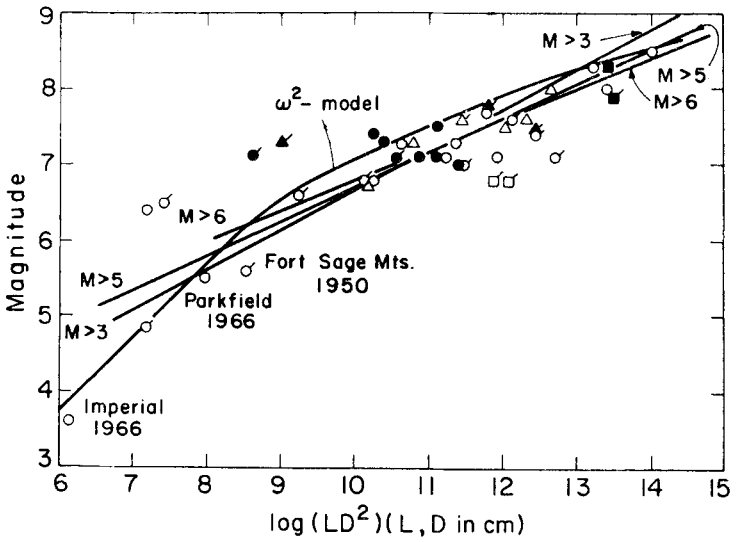

FIG. 3. The product of fault length L and the square of offset D as a function of magnitude reproduced from King & Knopoff (1968), with the additional curve for the ω-square model.

from King & Knopoff (1968), where L is the fault length and D is the fault offset. King & Knopoff found that the slope of best-fitting lines is significantly different from the slope of any published magnitude-seismic energy relations. From this result, assuming a dislocation model with a constant efficiency independent of magnitude, they concluded low fractional stress-drop for small earthquakes. Their conclusion has been extended to small earthquakes by Wyss (1970), and was considered as an evidence against the similarity assumption (constant stress-drop) underlying the ω-square model.

The parameter LD^2 is proportional to L^3, and therefore to the seismic moment in the ω-square model. One can draw a theoretical relation between M_s and LD^2 by finding the seismic moment for a given M_s in Fig. 1 and multiplying a constant. For a rectangular fault with width W, this constant is equal to $D/\mu W$, which is a measure of strain-release or stress drop. The constant was chosen as 3×10^{-17} dyne^{-1} cm^2 in Fig. 3. Assuming that $\mu = 3\times10^{11}$ dyne cm^{-2} in the Earth's crust, we find that $D/W = 10^{-5}$ and $\mu(D/W) = 3$ bars. Since most observed points for large earthquakes lie below our curve in Fig. 3, the correct ratio of LD^2 to moment may be 10 times larger than 3×10^{-17} dyne^{-1} cm^2. Then $D/W = 10^{-4}$ and $\mu(D/W) = 30$ bars. These values are reasonable rough estimates of stress drop in large shallow earthquakes (Chinnery 1964; Brune & Allen 1967). A recent summary of earthquake mechanism studies by Aki (1972) demonstrates that the stress drop in shallow earthquakes with $M > 6$ is 10–100 bars independent of magnitude. Here, again, we see that the ω-square model can explain observed field data on large earthquakes.

(3) *Seismic moment*

Fig. 4 is reproduced from Aki (1972), who summarized the data on M_s and seismic moment obtained from long-period surface waves and free oscillations. Body wave results were not included because of the controversial window effect discussed by Linde & Sacks (1971), who concluded that theories which predict constant displacement spectrum for body waves at long periods (the ω-square model is one of them)

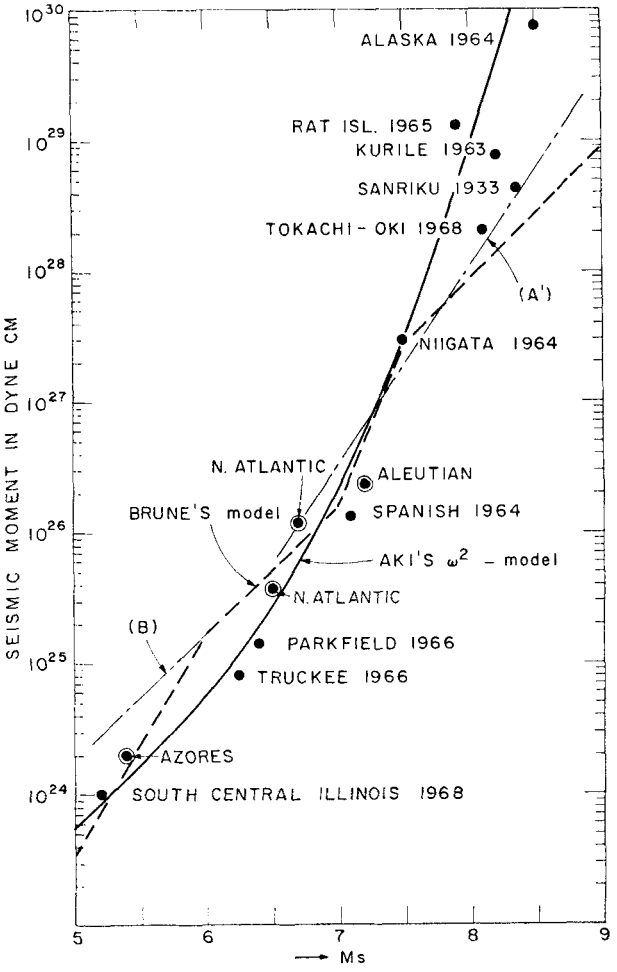

FIG. 4. Seismic moment as a function of magnitude reproduced from Aki (1972) with additional lines (A') and (B) for the ω-model of Brune & King (1967) as described in text.

must be in error. Their results are in favour of the Archambeau (1968) theory which predicts a sharp drop of spectrum toward zero frequency. We disagree with their conclusion because the surface wave and free oscillation spectra which do not suffer from the window effect invariably show consistency with the assumption of step function dislocation at the low-frequency end of observable spectrum. The best example is the free oscillation amplitude excited by the Kurile earthquake of 1963 October 13 ($M = 81/4$). Abe (1970) demonstrated that the assumption of step function was valid for the order numbers 10–30 for both spheroidal and torsional oscillations. Other convincing cases may be found in Ben-Menahem & Toksöz (1963), Aki (1966), Kanamori (1970a, b), Tsai & Aki (1969, 1970a, b, 1971).

The smooth curve designated as ' ω^2-model ' in Fig. 4 was drawn by plotting the height of the flat portion of spectrum for a given M_s shown in Fig. 1. The absolute value was fixed in such a way that the curve passes through the observed point for the Niigata earthquake, for which the first accurate determination of seismic moment was made by Aki (1967).

The dashed lines in Fig. 4 represent the calibration curve used by Brune (1968) and Davies & Brune (1971) to find the rate of slip along major fault zones of the Earth from the earthquake magnitude data. The curve was developed through a series of papers by Brune and his colleagues (Brune & King 1967; Brune & Engen 1969; Wyss & Brune 1968), and consisting of the following line segments:

(A) $\log M_0 = M_s + 19{\cdot}9$ for $M_s > 7{\cdot}5$ and strike slip. (0·3 is added for dip slip)

(B) $\log M_0 = M_s + 19{\cdot}2$ for $7 > M_s > 6$

(C) $\log M_0 = 1{\cdot}4M_L + 17{\cdot}0$ for $6 > M_L > 3$

The segments (A) and (B) were originally proposed by Brune & King as a relation between M_s and the Rayleigh wave amplitude at about 100-s periods. They assumed ω^{-1}-dependence instead of ω^{-2}, and using Tocher and Iida's data on fault length, assumed that the corner period is longer than 100 s for $M_s > 7{\cdot}5$, and is shorter than 20 s for $M_s < 7$. Thus, the constants in (A) and (B) differ by the logarithm of the ratio of two periods, as can be figured out from a schematic illustration of scaling law for the 'ω-model' shown in Fig. 5. It is obvious from Fig. 5 that the coefficient in the moment-magnitude relation for $M > 7$ should be 1·5 and cannot be unity as given in (A). In order to be consistent with the model described by Brune & King (1967), we must replace the formula (A) by the following:

(A′) $$\log M_0 = 1{\cdot}5M_s + 16{\cdot}0, \text{ for } M > 7$$

This will connect to the line (B) properly as expected for the ω-model sketched in Fig. 5.

Since the formula (C) was obtained empirically as the relation for local magnitude M_L, it is not applicable to the data shown in Fig. 4. Formula (B) should apply to all M_s less than 6 as can be seen from Fig. 5. If we compare the data in Fig. 4 with the formulas (A′) and (B) shown by chained lines, we find a systematic discrepancy; all

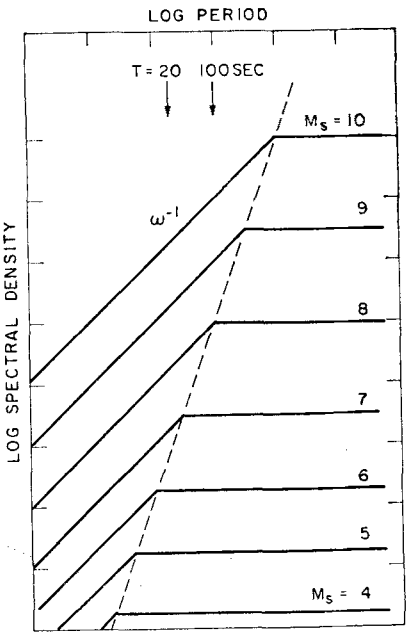

FIG. 5. Schematic representation of the scaling law of seismic spectrum based on the ω-model of Brune & King (1967).

the data for $M_s < 6{\cdot}5$ fall below line (B), and all the data for $M_s > 7{\cdot}5$ lie above line (A'). On the other hand, the ω^2-model explains the observation without significant systematic error with few exceptions like the Sanrika earthquake.

It is true, however, that Brune–King's ω-model explains the mantle wave data of Brune & King (1967) and Brune & Engen (1969) somewhat better than the ω-square model. Most of their data on large earthquakes are, however, from old instruments, and Brune and Engen express some concern about uncertain instrument calibration. Furthermore, the correction for attenuation and geometrical spreading may be biased because most of the data for small earthquakes are from the Pasadena station and larger ones are from other stations. Such problems may be avoided by the use of spectral ratio between earthquakes with different size but with common path and recording station.

(4) *Spectral ratio*

The observed seismic spectrum is a function of source, path and receiver. The simplest way of isolating the source spectrum is to compare seismograms obtained by the

FIG. 6. Locations of earthquake pairs with spectral ratios consistent with the ω-square model (designated by solid circles) and those inconsistent (designated by crosses). The events in China, Halmahera, and the Aleutians were studied by Tsujiura (1972) and the rest were studied by Berckhemer (1962) and Aki (1967).

same seismograph at the same station from two earthquakes of the same epicentre but of different size. Berckhemer (1962) was able to collect six such earthquake pairs from the Stuttgart records for the period 1931–1951. Their magnitudes range from 4·5 to 8·0, and the epicentral distances 400–9000 km. The separation between epicentres of each pair was less than 1°. Their locations are shown in a world map in Fig. 6. The ω-square model explains very well the observed spectral ratio for all the pairs, except the one in the Alps for which the comparison was fair (Aki 1967). A good agreement was obtained also for two aftershocks of the Kern County, California earthquake of 1952.

A similar collection of spectra for earthquake pairs has been made recently by Tsujiura (1972), using his multi-channel band-pass seismographs (Tsujiura 1966, 1967, 1969). The location of earthquake pairs is shown in Fig. 6. The ω-square model explained the spectral ratio for the pairs in China (M7·5/M6·1) and Halmahera (M7·2/M6·3) excellently. However, a striking discrepancy was found for two pairs of earthquakes in the Aleutians (M7·1/M6·3, M7·0/M5·7). Judging from their epicentres, they all belong to the underthrusting rather than the extensional group (Stauder 1968). Tsujiura's observation indisputably shows that the M7 and M6 Aleutian earthquake share nearly identical spectral shape in the period range 10–100 s. This result definitely contradicts the prediction of the ω-square model, because, as shown in Fig. 1, the corner period is about 10 s for $M = 6$, and about 40 s for $M = 7$.

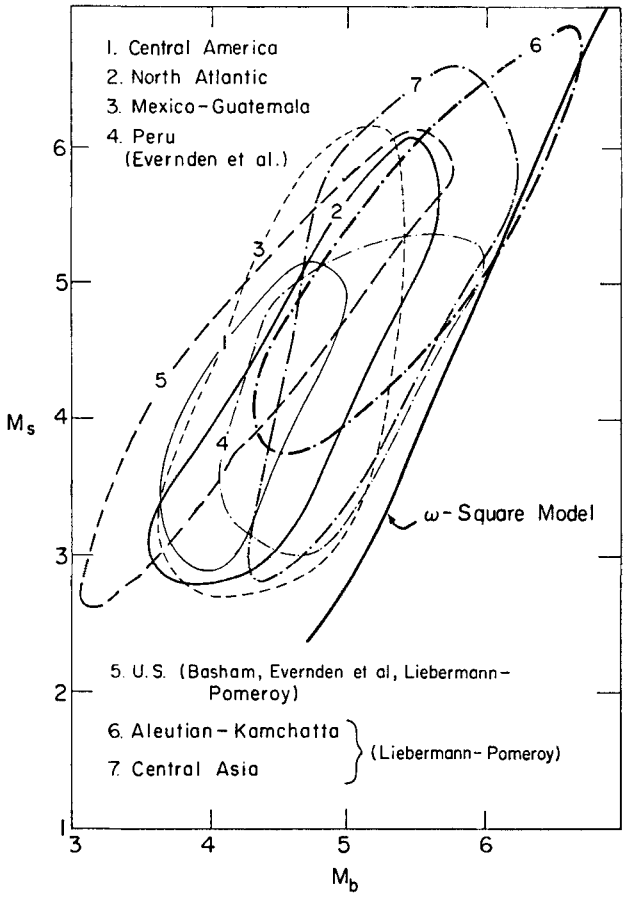

FIG. 7. Comparison of observed $M_s - M_b$ relation with the one predicted for the ω-square model.

So far, the failure of the ω-square model in explaining the scale effect on seismic spectrum may be considered as an exception. Such exceptional cases are the seismic moment of the Sanriku earthquake and the spectral ratios of the two earthquake pairs in the Aleutians. So far, we have considered the period range longer than 10 s. Once we enter the period range shorter than 10 s, however, the failure of the ω-square model becomes a rule rather than an exception.

(5) *$M_s - M_b$ relation*

Gutenberg & Richter (1956) discovered a discrepancy between the magnitude scale based upon short-period body waves (M_b) and that based upon long-period surface waves (M_s). This discrepancy was attributed to the scale effect by Aki (1967), and it was shown that the ω-square model explains the $M_s - M_b$ relation observed by them.

Recently, the $M_s - M_b$ relation attracted the attention of several seismologists because of its power as a discriminant between earthquakes and underground explosions (Liebermann *et al.* 1966; Liebermann & Pomeroy 1967, 1969; Capon, Greenfield & Lacoss 1967; Basham 1969; Molnar *et al.* 1969; Evernden *et al.* 1971; Liebermann & Basham 1971).

Fig. 7 summarizes the range of observed data on M_s *vs.* M_b for various regions. The curve designated as 'ω-square model' is drawn assuming that M_s is proportional to the spectral density at the period 20 s, and M_b is proportional to that at 1 s. The former assumption is valid because of the definition of M_s, and the latter is valid because the response of seismographs used for teleseismic P waves from small events are usually sharply peaked at about 1 s. This assumption was used by Liebermann & Pomeroy (1969) in their discussion of the $M_s - M_b$ relation. Aki (1967) took into account the small effect of signal duration as shown in Fig. 8 for larger events, but

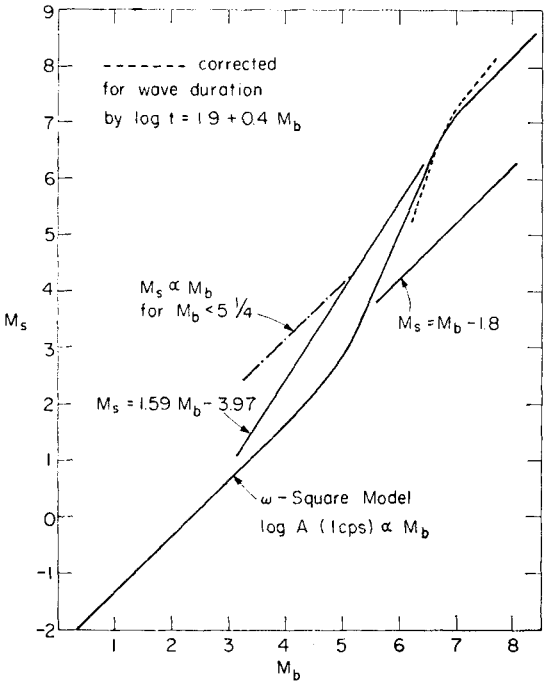

FIG. 8. Theoretical $M_s - M_b$ relation for the ω-square model as compared with empirical formulas of Gutenberg–Richter (1956) and Evernden *et al.* (1971) for earthquakes and that of Thirlaway–Carpenter (1966) for explosions.

such correction may be unnecessary for smaller events, for which the duration is probably determined by the instrument response and path effect. The curve for the ω-square model is further restricted to pass through the point ($M_s = M_b = 6\frac{3}{4}$) according to the original definition by Gutenberg & Richter (1956).

Fig. 7 clearly demonstrates that the observed $M_s - M_b$ relation deviates systematically from the predicted for the ω-square model. The data follow the straight linear extrapolation of the Gutenberg–Richter formula ($M_s = 1{\cdot}59M_b - 3{\cdot}97$) rather than following the bended curve of the ω^2-model as shown in Fig. 8. It is extremely interesting to note that this departure from the ω-square model makes the discrimination between explosion and earthquake possible for small events. The data for explosions are represented by a line $M_s = M_b - 1{\cdot}8$, which was established by Thirlaway & Carpenter (1966).

The fact that the $M_s - M_b$ relation for earthquakes does not bend according to the ω-square model but follows the straight line along the extrapolated Gutenberg–Richter formula has an additional support from a work on spectral densities done in the U.S.S.R. Chalturin (1970) made observations at Garm, using a multi-channel band-pass seismograph similar to Tsujiura's (1966, 1967, 1969), and found that the observed relation between the amplitudes at 1 s and 20 s follows a straight line with the coefficient the same as in the Gutenberg–Richter formula, and does not agree with the prediction of the ω-square model. This evidence is particularly strong because no assumptions are made on the relation between magnitudes and spectral densities.

Evernden *et al.* (1971) emphasize the parallelism of the M_s *vs.* M_b curves for explosions and earthquakes, and suggest that the $M_s - M_b$ relation for earthquakes with $M_b < 5\frac{1}{4}$ has a slope of approximately 1. Such a suggestion is not inconsistent with the observation, but the data show too much scatter to allow a firm conclusion (see Figs 7 and 8).

3. Revised models

Since the ω-square model explains, in general, the observations for the period range longer than 10 s, the right half of Fig. 1 should be left unchanged. In order to revise the left half, we shall consider the following two extreme cases. In one revision, we shall keep the ω^{-2}-dependence, but discard the similarity assumption and change the relation between M_s and the corner frequency. This shall be called the revised model A. In the other, we shall give up the ω^{-2}-dependence and adopt the ω^{-1}-dependence in the period range between 10–0·01 s. In this case, the relation between M_s and the corner period is unchanged from the ω-square model. We shall refer to this as the revised model B.

(1) *Model A*

Fig. 9 shows the family of spectral curves for the revised model A, in which the spacing between the curves of Fig. 1 at 1 s was widened to satisfy observed $M_s - M_b$ relation (following the Gutenberg–Richter formula down to $M_b = 5\frac{1}{4}$ and then switching to the line proposed by Evernden *et al.* (1971)) without changing the ω^{-2}-dependence. This resulted in a shift of corner period to the right for $M_s < 6$. For $M_s < 4\frac{1}{2}$, the corner period stays constant, because we follow the suggestion of Evernden *et al.* (1971) that the slope of the $M_s - M_b$ relation is unity for $M_b < 5\frac{1}{4}$.

The relation between M_s and the corner frequency is shown in Fig. 10 for various cases. The one corresponding to the suggestion of Evernden *et al.* indicates the corner period of about 6 s for $M_s < 4\frac{1}{2}$. The physical picture behind this is very simple. The fault length, rupture propagation time, and rise time are common to all the earthquakes smaller than $M_s < 4\frac{1}{2}$. The only difference between them is the offset, or strain release or stress drop. This is a revival of Benioff's (1951) idea mentioned in the introduction, and was suggested by Brune & Wyss at the Woods

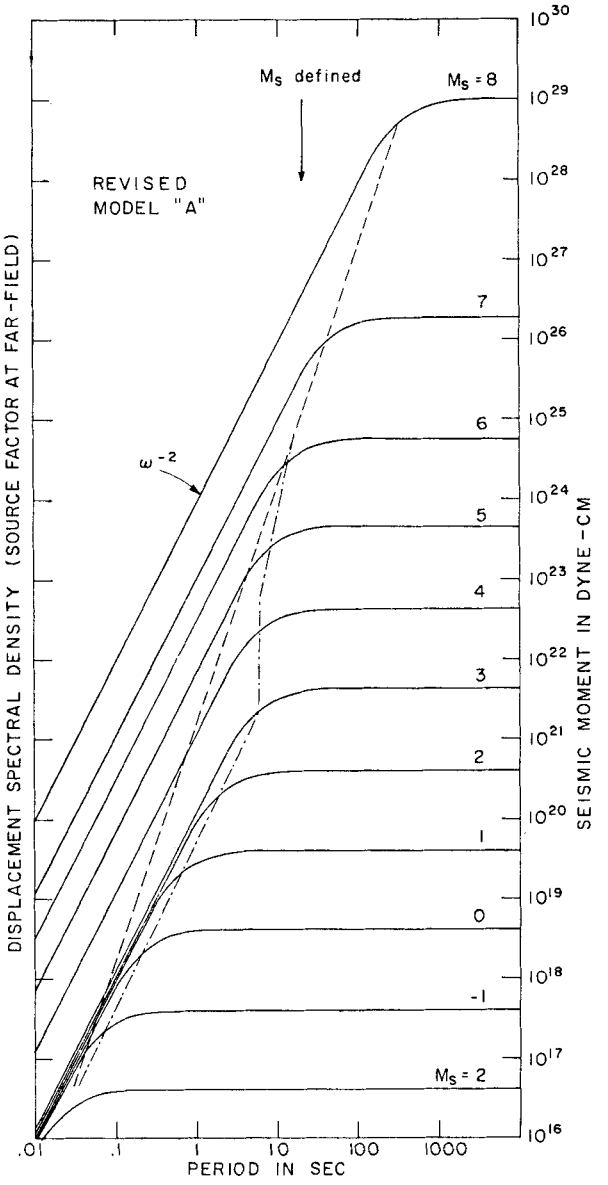

FIG. 9. Source factor of far-field seismic spectral density from earthquakes with various M_s for the revised model A.

Hole Conference on Seismic Discrimination July 1970, sponsored by the Advanced Research Projects Agency. This idea is quite compatible with the concept of 'pre-existing fault' which naturally violates the assumption of similarity.

One cannot, however, extend the 6-s corner period to microearthquakes ($M \simeq 0$). The frequency ranges of usual microearthquakes are between 10 to 100 cps (Nevada may be an exceptional area according to Douglas & Ryall (1972), and Takano (private communication)). For example, typical records of microearthquakes may be found in Furuya (1969), and an extensive collection of data in Terashima (1968).

Although M_s cannot be used for microearthquakes, the seismic moment has been estimated for the magnitude zero earthquake by Wyss & Brune (1968), Aki (1969),

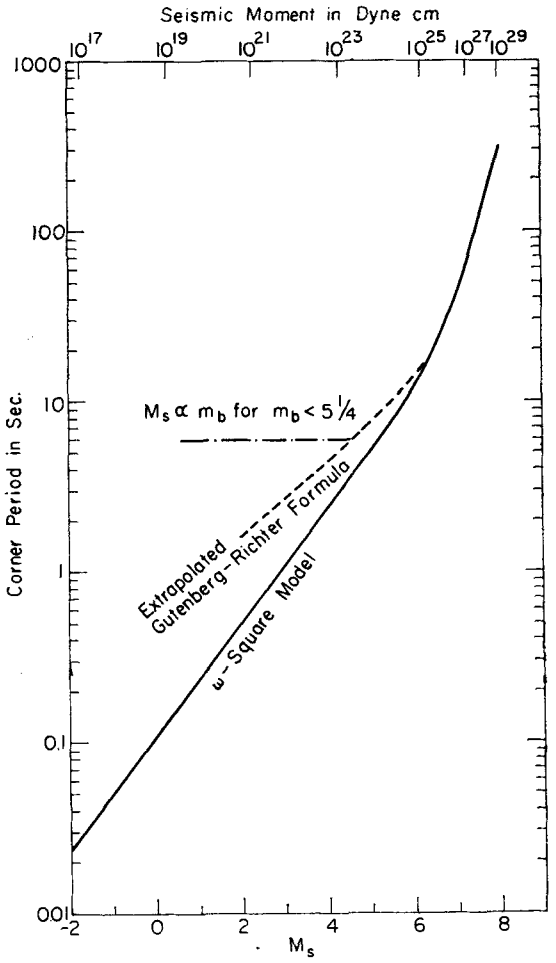

FIG. 10. Theoretical M_s versus corner-frequency relation for the ω-square model as compared with those implied by the $M_s - M_b$ relations of Gutenberg–Richter (1956) and Evernden *et al.* (1971).

Takano (1971a, b) and Douglas & Ryall (1972) as $10^{16} \sim 10^{17}$ dyne cm. Therefore, the actual corner period should reach the vicinity of the lower-left corner of Fig. 10. The curve for the ω-square model does, but others have to be sharply bent to reach that corner. Such a sharp bend in the corner period curve produces a strange scaling law of spectrum for $M_s < 3$ as shown in Fig. 9. All the earthquakes with $-1 < M_s < 3$ share the same spectral density for frequencies higher than 20 cps.

Both the bend in the magnitude-corner period relation and the above mentioned peculiar scaling law of microearthquake spectrum are demonstrated in the data reported by Terashima (1968) (see his Figs 5.5 and 6.5). Unfortunately, the definitions of magnitude and corner period are different between large and small earthquakes, and it is impossible to decide whether the apparent bend in the M_s-corner period curve reported by Terashima is due to the scale effect or some other effects such as a gap in recording instrument response for large and small earthquakes, or different attenuation and wave scattering effects between short and long periods.

It is, nevertheless, intriguing to consider the earthquake of revised model A as consisting of three distinct groups: one with $M_s > 6$, one with $6 > M_s > 3$, and the other with $M_s < 3$. The largest earthquake group has roughly constant stress drop

(10 to 100 bars) independent of earthquake magnitude. The medium-sized group shares pre-existing faults (a few kilometres long), and the smaller shock of this group shows less stress drop. In the smallest group, on the other hand, the stress drop increases with the decreasing magnitude, in agreement with Mogi's (1962) observation on the size effect on fracture strength and with the high stress drop observed in laboratories for small rock samples (the fracture strength is proportional to $L^{-0.1}$ where L is the linear dimension of the sample, according to Mogi). If the Earth's crust contains weak zones, faults or cracks of a size predominantly a few kilometres, it is conceivable to have such distinct groups of earthquakes.

(2) *Model B*

Let us consider the other extreme way of modifying the ω-square model. Keeping the M_s *vs.* corner-frequency curve unchanged, and simply changing the frequency dependence from ω^{-2} to ω^{-1} for periods less than about 5 s, we can approximately satisfy the observed $M_s - M_b$ relation. Since the ω^{-1} dependence up to the infinite frequency results in an infinite seismic energy, we assume that the spectral density drops sharply at about 100 cps. The resultant family of spectral curves is shown in Fig. 11.

This set of curves also explain all the main observations discussed earlier: (1) fault length, (2) stress drop, (3) seismic moment, (4) spectral ratio for $T > 10$ s, and (5) $M_s - M_b$ relation. In this modification, we assumed that the suggested bend of M_s *vs.* corner frequency may not be due to the source effect but due to instrumental or propagational path effects. Thus, the M_s—corner frequency relation is the same straight line as in the ω-square model.

One additional support of this model comes from the work of Asada & Takano (1963) and Takano (1970, 1971a, b) on the attenuation measurement using the spectral shape in the period range 0·1–1 s. They assumed the ω^{-1} dependence at the source and obtained reasonable Q values. They used this shape of source spectrum following Kanai & Yoshizawa's (1958) classic work on the seismic spectrum of nearby earthquakes measured in a deep mine in Japan.

Instead of three groups of earthquakes for revised model A, we find two distinct groups for model B. Earthquakes with $M_s < 6$ are all the same kind; the ω-model of Brune & King (1967) discussed earlier. On the other hand, earthquakes with $M_s > 6$ have peculiar spectral shapes. For example, the spectrum for M8 first decreases as ω^{-2} beyond the corner frequency (about 0·003 cps) but then the decrease slows down to ω^{-1} beyond 0·1 cps.

Within the scheme of a simple dislocation model of an earthquake described by a unidirectional rupture propagation and a step-like slip with a finite rise time (Haskell 1964), the above ω-model implies a very short rise time, outside the range of seismological observation. In view of an incoherent rupture propagation such as described by Haskell (1966) and Aki (1967), the ω-model may correspond to a process in which the fault offset takes place as a succession of irregular rapid motion with a very short time constant. In other words, the fault moves like a car running at a full speed on a very bumpy road. Finally, in the framework of Brune's (1970) model, the ω-model implies very small fractional stress drop, or very large difference between dynamic and static friction. These three interpretations appear to describe the same phenomena: rapid slips and sudden stops.

The peculiar spectral shape for large earthquakes may be explained, if the large one behaves as an ω-model up to a certain size, then transforms into an ω-square model. It seems reasonable to consider that rough and bumpy fault planes of the ω-model become smooth for larger displacements and produce faulting in accordance with the ω-square model which explains the geologic observations on earthquake faults.

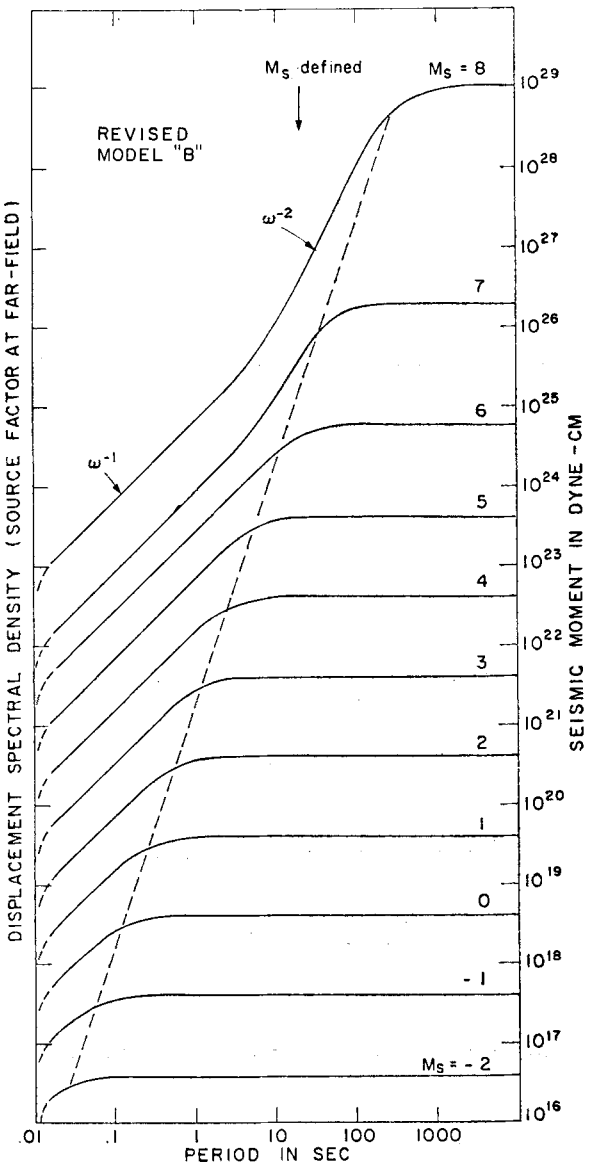

FIG. 11. Source factor of far-field seismic spectral density from earthquakes with various M_s for the revised model B.

As mentioned before, the ω-square model failed to explain Tsujiura's observation on two Aleutian earthquake pairs with magnitudes M_s 5·7 to 7·0. The model predicted a spectral ratio change of almost 10 times from 10 to 100 s, while the observed showed a very small change, with a nearly constant value over the same period range. In terms of the revised model A, this result means that all these earthquakes probably had fault planes of the same size. This observation may be approximately explained by the revised model B, if the transition from a rough faulting to a smooth one takes place at larger displacements or for a larger fault size in the Aleutians than in other parts of the world.

Working models such as A and B, which predict the scaling effect on seismic spectrum over the complete frequency range and dynamic range of earthquake

seismology, will relate observations on large earthquakes with those on small ones, and the observations at low frequencies with those at high frequencies.

4. Scaling law of dislocation time-function

The source factor $A(\omega)$ of the far-field seismic spectrum can be written in terms of the fault-slip $D(\bar{\xi}, t)$, or the displacement discontinuity, specified as a function of time t and the point $\bar{\xi}$ on the fault plane Σ as follows (Haskell 1964):

$$A(\omega) = \int_{\Sigma}\int \dot{D}(\bar{\xi}, \omega) \exp\left[-i(\omega r/\alpha)\right] d\Sigma_{\xi} \tag{1}$$

where $\dot{D}(\bar{\xi}, \omega)$ is the Fourier transform of the fault-slip velocity $\dot{D}(\bar{\xi}, t)$, r is the distance to the observer from the surface element $d\Sigma_{\xi}$, and α is the velocity of waves.

At low frequencies, where the change of $\omega r/\alpha$ within Σ is negligible, the far-field spectrum is simply proportional to the spectrum of fault-slip velocity integrated over the fault plane. Therefore, the average value of dislocation velocity spectrum may be obtained by dividing $A(\omega)$ by the fault area.

For the inversion at higher frequencies, we shall assume a simple model of one-dimensional rupture propagation, such as considered by Ben-Menahem (1961), Haskell (1964) and Aki (1967). In that case, equation (1) is replaced by

$$A(\omega) = W \int_{0}^{L} \dot{D}(\xi, \omega) \exp\left[-i(\omega r/\alpha)\right] d\xi \tag{2}$$

where ξ is the co-ordinate along the path of rupture propagation, L is the final fault length, W is the width, and fault-slip $D(\xi, \omega)$ is considered as the average value over the width.

For a uniform slip motion with constant propagation velocity used by Ben-Menahem (1961),

$$\dot{D}(\xi, t) = \dot{D}\left(t - \frac{\xi}{v}\right)$$

and therefore,

$$\left.\begin{aligned} A(\omega) &= W \int_{0}^{L} \dot{D}(\omega) \exp\left[(-i\omega\xi/v) - i(\omega r/\alpha)\right] d\xi \\ |A(\omega)| &\doteqdot |\dot{D}(\omega)| . WL . \frac{\sin x}{x} \end{aligned}\right\} \tag{3}$$

where $x = L\omega/2(1/v - \cos\theta/\alpha)$, and θ is the angle between the ξ-axis and the direction to the observer. For high frequencies, therefore, the far-field spectrum is proportional to the fault area, the fault-slip velocity spectrum and roughly to ω_0/ω, where ω_0 is $2/[L(1/v - \cos\theta/\alpha)]$; a measure of corner frequency for the model. The same result is obtained for the incoherent propagation models used by Haskell and Aki, for frequencies beyond the corresponding corner frequency. Thus, on the assumption of one-dimensional rupture propagation, one can obtain the spectrum of fault-slip velocity at frequencies higher than the corner frequency ω_0 by dividing the far-field spectrum by the fault area and multiplying it by ω/ω_0.

The validity of the above procedure should be subject to future critical investigations. If the rupture propagation is two-dimensional as considered by Berckhemer (1962), Hirasawa & Stauder (1965) and Savage (1965), one should expect ω^{-2} effect beyond the corner frequencies. In that case, the correction should be

multiplying $(\omega/\omega_0)^2$, instead of ω/ω_0. Of course, the two-dimensional propagation is more realistic because a fault is not a line but a plane. I feel strongly, however, that one of the corner frequencies must be much higher than the frequencies associated with the total time of rupture propagation and the rise time of fault slip, because otherwise, we expect that the ω-cube model explains the observation on the $M_s - M_b$ relation, but it does not (Aki 1967). The second corner frequency of rupture propagation may be associated with a very short transient time of starting and stopping a primarily one-dimensional rupture propagation.

Now let us apply our tentative procedure of inversion to the far-field spectrum and find the scaling law of fault-slip time-function. The spectral densities at low frequencies shown in Figs 1, 9 and 11 are divided by the fault area (the square of the corner period). For frequencies higher than the corner frequency, an additional multiplication by a factor proportional to ω/ω_0 is applied. The resultant family of spectral curves for the fault-slip velocity spectrum are shown in Fig. 12, 13 and 14, respectively for the ω-square model, revised model A and B.

It is remarkable that the absolute value of spectra density of dislocation velocity at periods shorter than 5 seconds is independent of magnitude for earthquake with $M_s > 6{\cdot}5$ for all three models.

According to Haskell's (1969) calculation on the elastic near-field of fault motion, not only the maximum displacements but also the maximum velocity and acceleration takes place in the immediate vicinity of the fault plane. According to Aki's (1968) similar calculation, the seismic motion near a fault depends neither on fault length nor on fault width once they exceed certain limits, but is determined mostly by the dislocation time-function and velocity of rupture propagation. Since the rupture velocity is apparently independent of earthquake magnitude, we must conclude that the maximum seismic motion associated with an earthquake scales as the fault-slip time-function.

Then, our results on the scaling law of fault-slip time-function will have an important effect on earthquake engineering, because they imply that the maximum seismic motion of an earthquake in the period range less than 5 s is a constant independent of magnitude for $M_s > 6{\cdot}5$.

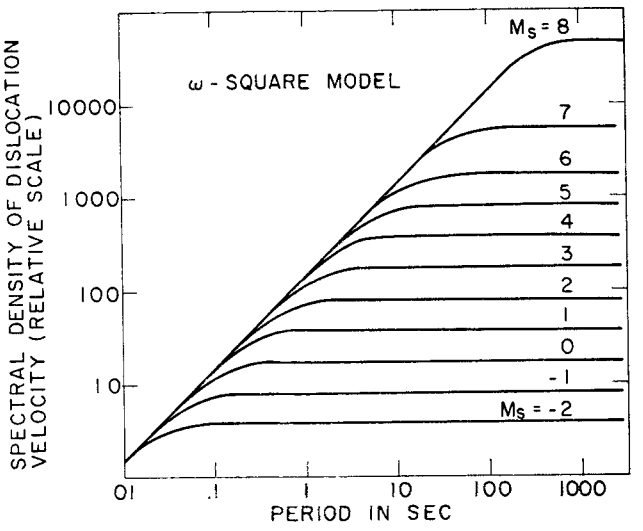

FIG. 12. Spectral densities of dislocation velocity (velocity of fault-slip motion) for different M_s based on the ω-sqauare model.

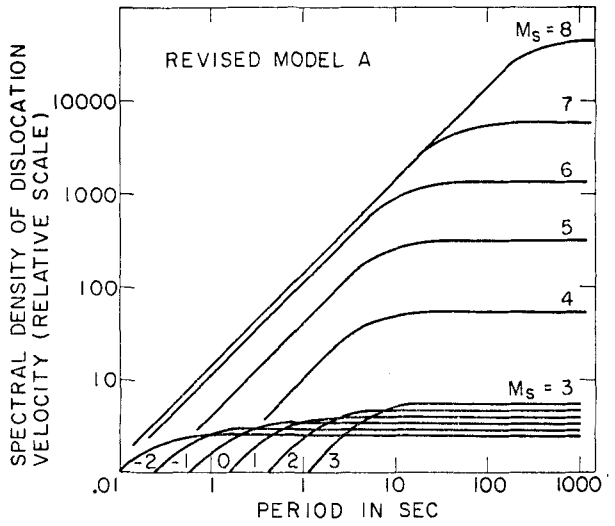

FIG. 13. Spectral densities of dislocation velocity (velocity of fault-slip motion) for different M_s based on the revised model A.

It must be emphasized here that the above conclusion is supported only indirectly by observations. No mention has been made of any group of observations applying to the upperleft quarter of Figs 1, 9 and 11. The waves in this quarter are short waves coming from large earthquakes. They suffer not only from the complexity of a large source, but also from the complex path effect on short waves, and this makes the interpretation of the seismogram extremely difficult. Because of this difficulty, they have not attracted due attention. Housner (1955) considered a swarm of pulses random in time resulting from release of shear dislocations distributed randomly over a fault plane. Haskell (1964) introduced incoherent rupture propagation in order to account for observations on short waves from a large earthquake. The concept

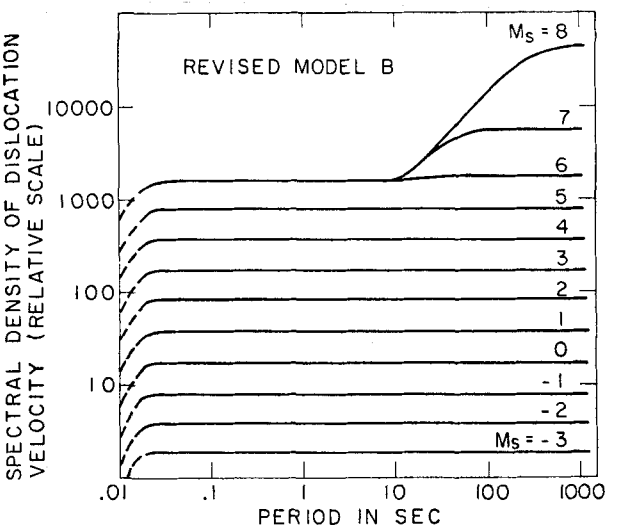

FIG. 14. Spectral densities of dislocation velocity (velocity of fault-slip motion) for different M_s based on the revised model B.

of a ' multiple shock ' is an old idea introduced to explain this most complex portion of a seismogram (Stoneley (1937), Usami (1956), Wyss & Brune (1967), Trifunac & Brune (1970), among others). Miyamura *et al.* (1965) summarize observations and discuss physical mechanisms.

The idea of a ' multiple shock ' implies that a large earthquake consists of a sequence of several small earthquakes occurring within the epicentral region. One must realize, however, the extremely large value of seismic moment for the largest earthquakes. For example, the Alaska earthquake of 1964 ($M = 8{\cdot}5$, $M_0 = 7{\cdot}5 \times 10^{29}$ dyne cm) can be a multiple of several Rat Island earthquakes of 1965 ($M = 7{\cdot}9$, $M_0 = 1{\cdot}2 \times 10^{29}$), but requires about 10 000 San Fernando earthquakes of 1971 ($M = 6{\cdot}6$, $M_0 = 7{\cdot}5 \times 10^{25}$). The ' multiple shock ' model of a large earthquake will also have a scale effect on the spectrum; the spectrum at periods longer than the total duration of faulting will increase proportionally with the number N of component events, but the high frequency spectrum will be proportional to $\sqrt{N}$ because of random interference. Thus, the spectral ratio between large and small earthquakes at low frequency will be the square of the ratio at high frequencies. This scale effect is the same as that of the ω-model of Brune & King (see Fig. 5). As discussed earlier, observations for large earthquakes are in favour of the ω-square model, which predicts that the spectral ratio at low frequency is the cube of the ratio at high frequency. The idea of ' multiple shock ' for large earthquakes is not compatible with our revised model B, in which small earthquakes are described by the ω-model, but large ones by a composite model of ω and ω-square.

Note added on 1972 April 27

At the annual meeting of the Seismological Society of America in March, 1972, B. Tucker and J. N. Brune reported the observed relation between the corner frequency and seismic moment for aftershocks (magnitudes 0·5–4·2) of the San Fernando earthquake, February 1971. More recently, at the annual meeting of the American Geophysical Union, April, 1972, W. Thatcher and T. C. Hanks reported the same relation for earthquakes ($2 < M_L < 6$) in southern California. Although the data show large scatter, they agree with the predicted curve for the ω-square model and the revised model B shown in Fig. 10, but deviate from the predicted curve for the revised model A. We must, therefore, consider that the revised model A is unsatisfactory.

Acknowledgments

The author is grateful to Dr M. Tsujiura of the Earthquake Research Institute, University of Tokyo, for his generosity in letting the author use his latest result before publication. Dr Kei Takano of the Geophysical Institute, University of Tokyo, kindly supplied the author with information on the recent developments in micro-earthquake studies in Japan.

This work was supported in part by the National Science Foundation under Grant GA 24268, and in part by the Advanced Research Projects Agency monitored by the Air Force Office of Scientific Research through contract F 44620-71-C-0049.

Department of Earth and Planetary Sciences,
Massachusetts Institute of Technology,
Cambridge, Massachusetts 02139.

References

Abe, K., 1970. Determination of seismic moment and energy from the earth's free oscillation, *Phys. Earth Planet. Int.*, **4**, 49–61.

Aki, K., 1966. Generation and propagation of G waves from the Niigata earthquake of June 16, 1964, *Bull. Earthq. Res. Inst., Univ. Tokyo*, **44,** 23–88.
Aki, K., 1967. Scaling law of seismic spectrum, *J. geophys. Res.*, **72,** 1217–1231.
Aki, K., 1968. Seismic displacements near a fault, *J. geophys. Res.*, **73,** 5359–5376.
Aki, K., 1969. Analysis of the seismic coda of local earthquakes as scattered waves, *J. geophys. Res.*, **74,** 615–631.
Aki, K., 1972. *Earthquake mechanism*, Proceeding of the Final UMP Symposium, ed. R. Ritsema, Moscow 1971.
Archambeau, C., 1968. General theory of elastodynamic source fields, *Rev. Geophys.*, **6,** 241–288.
Asada, T., 1957. Observations of nearby microearthquakes with ultra-sensitive seismometers, *J. Phys. Earth*, **5,** 83–113.
Asada, T. & Takano, K., 1963. Attenuation of short-period P waves in the mantle, *J. Phys. Earth*, **11,** 25–34.
Basham, P. W., 1969. Canadian magnitudes of earthquakes and nuclear explosions in south-western North America, *Geophys. J. R. astr. Soc.*, **17,** 1–13.
Båth, M. & Duda, S. J., 1964. Earthquake volume, fault plane area, seismic energy, strain, deformation and related quantities, *Ann. Geofis. Rome*, **17,** 353–368.
Benioff, H., 1951. Earthquakes and rock creep, Part I: creep characteristics of rocks and the origin of aftershocks, *Bull. seism. Soc. Am.*, **41,** 31–62.
Ben-Menahem, A., 1961. Radiation of seismic surface waves from finite moving sources, *Bull. seism. Soc. Am.*, **51,** 401–435.
Ben-Menahem, A. & Toksöz, M. N., 1963. Source mechanism from spectrum of long-period surface waves: 2. Kamachatka earthquake of November 5, 1952, *J. geophys. Res.*, **68,** 5207–5222.
Berckhemer, H., 1962. Die Ausdehnung der Bruchfläche im Erdbebenherd und ihr Einfluss auf das seismiche Wellenspektrum, *Gerlands Beitr. Geophys.*, **71,** 5–26.
Brune, J. N., 1968. Seismic moment, seismicity, and rate of slip along major fault zones, *J. geophys. Res.*, **73,** 777–784.
Brune, J. N., 1970. Tectonic stress and the spectra of seismic shear waves from earthquakes, *J. geophys. Res.*, **75,** 4997–5009.
Brune, J. N., Correction to ' Tectonic stress and the spectra of seismic shear waves from earthquakes ', *J. geophys. Res.*, **76,** 5002.
Brune, J. N., 1971. Seismic sources, fault plane studies and tectonics, *Trans. Am. geophys. Un.*, **52,** 178–187.
Brune, J. N. & Allen, C. R., 1967. A low-stress-drop, low-magnitude earthquake with surface faulting: The Imperial, California, earthquake of March 4, 1966, *Bull. seism. Soc. Am.*, **57,** 501–514.
Brune, J. N. & Engen, G., 1969. Excitation of mantle Love waves and definition of mantle wave magnitude, *Bull. seism. Soc. Am.*, **59,** 923–933.
Brune, J. N. & King, D. Y., 1967. Excitation of mantle Rayleigh waves of period 100 seconds as a function of magnitude, *Bull. seism. Soc. Am.*, **57,** 1355–1365.
Capon, J., Greenfield, R. J. & Lacoss, R. T., 1967. *Surface-versus body-wave magnitude results*, in Semiannual Technical Summary, Lincoln Laboratories, M.I.T., pp. 3–5, Lexington, Mass., June 30.
Chalturin, V. I., 1970. *Proceedings of European Eng. Seismological Commission*, September, Sofia, Bulgaria.
Chinnery, M., 1964. The strength of the earth's crust under horizontal shear stress, *J. geophys. Res.*, **69,** 2085–2089.
Davies, G. & Brune, J. N., 1971. Regional and global fault slip rates from seismicity, *Nature*, **229,** 101–107.
Douglas, B. M. & Ryall, A., 1972. Spectral characteristics and stress drop for microearthquakes near Fairview Peak, Nevada, *J. geophys. Res.*, **77,** 351–359.

Evernden, J. F., Best, W. J., Pomeroy, P. W., McEvilly, T. V., Savino, J. M. & Sykes, L. R., 1971. Discrimination between small-magnitude earthquakes and explosions, *J. geophys. Res.*, **76,** 8042–8055.

Filson, J. & McEvilly, T. V., 1967. Love wave spectra and the mechanism of the 1966 Parkfield sequence, *Bull. seism. Soc. Am.*, **57,** 1245–1257.

Furuya, I., 1969. Predominant period and magnitude, *J. Phys. Earth*, **17,** 119–126.

Gutenberg, B. & Richter, C. F., 1956. Earthquake magnitude, intensity, energy, and acceleration, 2, *Bull. seism. Soc. Am.*, **46,** 105–145.

Haskell, N., 1964. Total energy and energy spectral density of elastic wave radiation from propagating faults, *Bull. seism. Soc. Am.*, **56,** 1811–1842.

Haskell, N., 1966. Total energy and energy spectral density of elastic wave radiation from propagating faults, 2, A statistical source model, *Bull. seism. Soc. Am.*, **56,** 125–140.

Haskell, N., 1969. Elastic displacements in the near-field of a propagating fault, *Bull. seism. Soc. Am.*, **59,** 865–908.

Hirasawa, T. & Stauder, W., 1965. On the seismic body waves from a finite moving source, *Bull, seism. Soc. Am.*, **55,** 237–262.

Housner, G. W., 1955. Properties of strong ground motion earthquakes, *Bull. seism. Soc. Am.*, **45,** 197–218.

Ida, Y. & Aki, K., 1972. Seismic source time function of propagating longitudinal-shear cracks, *J. geophys. Res.*, **76,** in press.

Iida, K., 1959. Earthquake energy and earthquake fault, *J. Earth Sci., Nagoya Univ.* **7,** 98–107.

Iida, K., 1965. Earthquake magnitude, earthquake fault, and source dimensions *J. Earth Sci., Nagoya Univ.*, **13,** 115–132.

Kanai, K. & Yoshizawa, S., 1958. The amplitude and the period of earthquake motions, *Bull. earthq. Res. Inst.*, **36,** 275–293.

Kanamori, H., 1970a. Synthesis of long-period surface waves and its application to earthquake source studies—Kurile Islands earthquake of October 13, 1963. *J. geophys. Res.*, **75,** 5011–5027.

Kanamori, H., 1970b. The Alaska earthquake of 1964: Radiation of long-period surface waves and source mechanism, *J. geophys. Res.*, **75,** 5029–5040.

Kanamori, H., 1971. Seismological evidence for a lithospheric normal faulting—the Sanriku earthquake of 1933, *Phys. Earth Planet. Int.*, **4,** 289–300.

King, C. Y. & Knopoff, L., 1968. Stress drop in earthquakes, *Bull. seism. Soc. Am.*, **58,** 249–257.

Liebermann, R. C. & Basham, P. W., 1971. Excitation of surface waves by the Aleutian underground explosion Milrow (October 2, 1969), *J. geophys. Res.*, **76,** 4030–4034.

Liebermann, R. C., King, C. Y., Brune, J. N. & Pomeroy, P. W., 1966. Excitation of surface waves by the underground nuclear explosion Long Shot, *J. geophys. Res.*, **71,** 4333–4339.

Liebermann, R. C. & Pomeroy, P. W., 1967. Excitation of surface waves by events in Southern Algeria, *Science*, **156,** 1098–1100.

Liebermann, R. C. & Pomeroy, P. W., 1969. Relative excitation of surface waves by earthquakes and underground explosions, *J. geophys. Res.*, **74,** 1575–1590.

Liebermann, R. C. & Pomeroy, P. W., 1970. Source dimensions of small earthquakes as determined from the size of aftershock zone, *Bull. seism. Soc. Am.*, **60,** 879–896.

Linde, A. T. & Sacks, I. S., 1971. Errors in the spectral analysis of long-period seismic body waves, *J. geophys. Res.*, **76,** 3226–3336.

Miyamura, S., Omote, S., Teisseyre, R. & Vesanen, E., 1965. Multiple shocks and earthquake series pattern, *Bull. int. Inst. seism. earthq. Eng.*, **2,** 71–92.

Mogi, K., 1962. The influence of the dimensions of specimens on the fracture strength of rocks—comparison between the strength of rock specimens and that of the earth's crust, *Bull. earthq. Res. Inst., Univ. Tokyo*, **40,** 177–185.

Molnar, P., Savino, J., Sykes, L. R., Liebermann, R. C., Hade, G. & Pomeroy, P. W., 1969. Small earthquakes and explosions in western North America recorded by new high-gain, long-period seismographs, *Nature*, **224,** 1268–1273.

Otsuka, M., 1965. Earthquake magnitude and surface fault formation, *J. seism. Soc. Japan, Ser.* 2, **18,** 1–8.

Press, F., 1967. *Dimensions of the source region for small shallow earthquakes*, Proceedings of the VESIAC Conference on the Current Status and Future Progress for Understanding the Source Mechanism of Shallow Seismic Events in the 3 to 5 Magnitude Range.

Savage, J. C., 1966. Radiation from a realistic model of faulting, *Bull. seism. Soc. Am.*, **56,** 577–592.

Stauder, W., 1968. Tensional character of earthquake foci beneath the Aleutian trench with relation to sea-floor spreading, *J. geophys. Res.*, **73,** 7693–7701.

Stoneley, R., 1937. The Mongolian earthquake of 1931, August 10, *Brit. Ass. seism. Comm.*, 42*nd Rep.*, 5–6.

Takano, K., 1970. Attenuation of short period seismic waves in the upper mantle and its regional difference, *J. Phys. Earth*, **18,** 171–180.

Takano, K., 1971a. A note on the attenuation of short period P and S waves in the mantle, *J. Phys. Earth*, **19,** 155–164.

Takano, K., 1971b. Analysis of seismic coda waves of ultra microearthquakes in the Matsushiro area—a comparison with Parkfield, California, *J. Phys. Earth*, **19,** 209–215.

Terashima, T., 1968. Magnitude of microearthquake and the spectra of microearthquake waves, *Bull. int. Inst. seism. earthq. Eng.*, **5,** 31–108.

Thirlaway, H. I. S. & Carpenter, E. W., 1966. Seismic signal anomalies, travel times, amplitudes, and pulse shapes, Proceedings of the VESIAC Special Study Conference on Seismic Signal Anomalies, Travel Times, Amplitudes, and Pulse Shapes, Beaugency, France, October.

Tocher, D., 1958. Earthquake energy and ground breakage, *Bull. seism. Soc. Am.*, **48,** 147–152.

Tocher, D., 1960. *Movement on faults*, Proc. 2nd World Conf. Earthquake Engineering, **1,** 551–564.

Trifunac, M. & Brune, J. N., 1970. Complexity of energy release during the Imperial Valley, California, earthquake of 1940, *Bull. seism. Soc. Am.*, **60,** 137–160.

Tsai, Y. B. & Aki, K., 1969. Simultaneous determination of the seismic moment and attenuation of seismic surface waves, *Bull. seism. Soc. Am.*, **59,** 275–287.

Tsai, Y. B. & Aki, K., 1970a. Source mechanism of the Truckee, California earthquake of September 12, 1966, *Bull. seism. Soc. Am.*, **60,** 1199–1208.

Tsai, Y. B. & Aki, K., 1970b. Precise focal depth determination from amplitude spectra of surface waves, *J. geophys. Res.*, **75,** 5729–5743.

Tsai, Y. B. & Aki, K., 1971. Amplitude spectra of surface waves from small earthquakes and underground nuclear explosions, *J. geophys. Res.*, **76,** 39 0–3952.

Tsuboi, C., 1940. Isostasy and maximum earthquake energy, *Proc. Imp. Acad.*, **16,** 449.

Tsuboi, C., 1956. Earthquake energy, earthquake volume, aftershock area and strength of the earth's crust, *J. Phys. Earth*, **4,** 63.

Tsuboi, C., 1958. On seismic activities in and near Japan, *Contributions in Geophysics: in honour of Beno Gutenberg*, Pergamon Press Ltd, Oxford.

Tsuboi, C., 1965. A theoretical derivation of the magnitude-energy equation of earthquakes, $\log E = aM + b$, *Proc. Japan Acad.*, **41,** 588.

Tsujiura, M., 1966. Frequency analysis of seismic waves (1), *Bull. earthq. Res. Inst., Tokyo Univ.*, **44,** 873–891.

Tsujiura, M., 1967. Frequency analysis of seismic waves (2), *Bull. earthq. Res. Inst., Tokyo Univ.*, **45,** 973–995.

Tsujiura, M., 1969. Regional variation of P wave spectra (1), *Bull. earthq. Res. Inst., Tokyo Univ.*, **47,** 613–633.

Tsujiura, M., 1972. Spectrum of seismic waves and its dependence on magnitude (1), *Bull. earthq. Res. Inst., Tokyo Univ.*, in press.

Usami, T., 1956. Seismometrical study of Boso-oki earthquake of November 26, 1953, *Quart. J. Seismology* (Kenshin-Jiho) Japan Meteor. Agency, **21,** 3.

Wyss, M., 1970. *Observation and interpretation of tectonic strain release mechanisms*, Ph.D. Thesis, Calif. Inst. of Technology.

Wyss, M. & Brune, J. N., 1967. The Alaska earthquake of 28 March 1964: A complex multiple rupture, *Bull. seism. Soc. Am.*, **57,** 1017–1023.

Wyss, M. & Brune, J. N., 1968. Seismic moment, stress, and source dimensions for earthquakes in the California-Nevada region, *J. geophys. Res.*, **73,** 4681–4694.